High-frequency climate linkages between the North Atlantic and the Mediterranean during marine oxygen isotope stage 100 (MIS100)

Julia Becker,[1,2] Lucas J. Lourens,[1] and M. E. Raymo[3]

Received 13 April 2005; revised 28 February 2006; accepted 27 March 2006; published 15 July 2006.

[1] High-resolution records of Mediterranean and North Atlantic deep-sea sediments indicate that rapid changes in hydrology and climate occurred during marine oxygen isotope stage 100 (MIS100) (at ~2.52 Ma), which exhibits characteristics similar to late Pleistocene Dansgaard-Oeschger, Bond cycles and Heinrich events. As in the late Pleistocene, North Atlantic oceanographic and atmospheric changes were probably transmitted into the Mediterranean by some combination of surface water inflow and Atlantic-Mediterranean atmospheric pressure gradients. Our data suggest that the mechanism(s) responsible for sub-Milankovitch and millennial-scale climate oscillations were the same over at least the past 2.6 Ma, notwithstanding the transition from the 41-kyr-dominated glacial cycles of the late Pliocene to the 100-kyr cycles of the late Pleistocene.

Citation: Becker, J., L. J. Lourens, and M. E. Raymo (2006), High-frequency climate linkages between the North Atlantic and the Mediterranean during marine oxygen isotope stage 100 (MIS100), *Paleoceanography*, *21*, PA3002, doi:10.1029/2005PA001168.

1. Introduction

[2] Paleoclimate records indicate that the Earth's climate is unstable and has oscillated on Milankovitch to millennial timescales throughout the late Pliocene and Pleistocene. Millennial-scale changes are most prominently reflected in North Atlantic sea surface and Greenland air temperature proxy records. These records reveal distinct oscillations on millennial (1–3 kyr) timescales during the last glacial maximum, so-called Dansgaard-Oeschger (D-O) cycles, which culminated in large-scale ice rafting events known as Heinrich (H) events [*Heinrich*, 1988; *Bond*, 1992; *Broecker*, 1992; *Bond et al.*, 1993; *Dansgaard et al.*, 1993; *Bond et al.*, 1999]. The leading hypothesis links the cold phases of the D-O cycles and H events to a collapse of the Northern Hemisphere ice sheets, resulting in the injection of large volumes of meltwater to the source regions of North Atlantic Deep Water (NADW) formation. Subsequently, lowered surface water salinities lead to a reduction of the deep convection and hence a slowdown of the global thermohaline circulation (THC) [*Broecker*, 1997] accounting for lower temperatures observed at high latitudes. Climate fluctuations associated with D-O cycles and H events are found in climate archives all over the world [*Leuschner and Sirocko*, 2000; *Voelker et al.*, 2002]. However, the forcing of these events is controversial. Some authors relate H events to internal ice sheet oscillations forced by the interaction of large ice sheets with the underlying bedrock [*MacAyeal*, 1993; *Alley and MacAyeal*, 1994]. On the other hand, the presence of D-O and H-like fluctuations at times of relatively small Northern Hemisphere ice sheets, e.g., during the Holocene [*Marchitto et al.*, 1998], the obliquity-dominated glacial cycles of the late Pliocene or middle Pleistocene [*Raymo et al.*, 1998; *McIntyre et al.*, 2001], and before 2.7 Ma [*Ortiz et al.*, 1999; *Kleiven et al.*, 2002] argue against this binge-purge hypothesis. It was therefore supposed that the D-O climate perturbations are persistent features of Earth's climate, probably triggered by changes in solar activity [*Bond et al.*, 2001] and amplified in the presence of large ice sheets [*Raymo et al.*, 1992; *Wara et al.*, 2000; *McIntyre et al.*, 2001]. Furthermore, modeling experiments [*Clement et al.*, 1999; *Schmittner and Clement*, 2002] and tropical paleoclimate records [*Peterson et al.*, 2000; *Dannenmann et al.*, 2003] suggest that millennial-scale climate variability could be driven by low-latitude rather than high-latitude forcing mechanisms. These may include strong atmosphere-ocean feedbacks, such as changes in the equatorial wind system equivalent to long-term changes in El Niño – Southern Oscillation (ENSO), changes in the intensity of the Intertropical Convergence Zone (ITCZ) or monsoon variability [*Stott et al.*, 2002].

[3] A key region to study the influence of D-O cycles and H events at midlatitudes to low latitudes is the Mediterranean. Proxy data from the western Mediterranean reveal distinct short-term changes in sea surface temperature (SST) and deep water formation that were closely related to the D-O cycles and H events during the past 50 kyr [*Rohling et al.*, 1998; *Asioli et al.*, 1999; *Cacho et al.*, 1999, 2000]. These rapid changes in Mediterranean hydrography and THC are partly attributed to the direct influence of the inflowing Atlantic surface waters as well as by an atmospheric connection with the North Atlantic climate system, both

[1]Department of Earth Sciences, Faculty of Geosciences, Utrecht University, Utrecht, Netherlands.
[2]Now at School of Earth, Ocean and Planetary Sciences, Cardiff University, Cardiff, UK.
[3]Department of Earth Sciences, Boston University, Boston, Massachusetts, USA.

0883-8305/06/2005PA001168$12.00

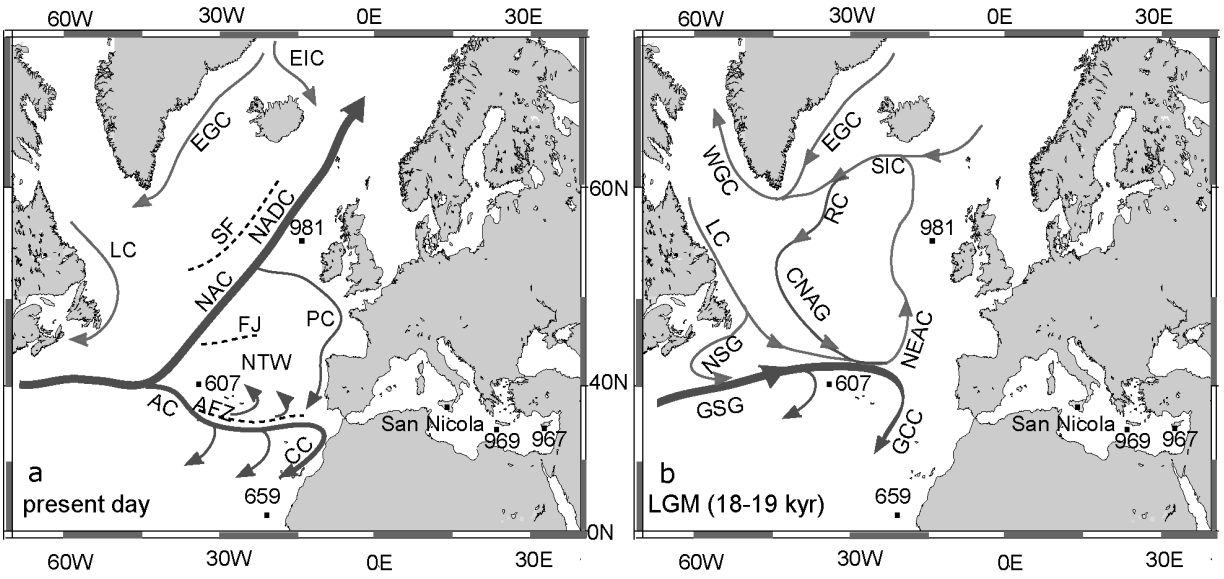

Figure 1. (a) Location map of Ocean Drilling Program (ODP) Site 981, Deep Sea Drilling Project (DSDP) Site 607, Monte San Nicola section, and ODP Site 967. Arrows indicate North Atlantic surface water masses: AC, Azores Current; CC, Canary Current; NTW, North Atlantic transitional waters; NAC, North Atlantic Current; PC, Portuguese Current; EIC, East Island Current; EGC, East Greenland Current; and LC, Labrador Current. Dashed lines indicate frontal zones: AFZ, Azores Frontal Zone; SF, Subpolar Front; and FJ, Frontal Jets. (b) Reconstruction of North Atlantic surface circulation during the Last Glacial Maximum (LGM) (18–19 kyr), redrawn from *Robinson et al.* [1995]. Abbreviations are GSG, Glacial Subtropical Gyre; GCC, Glacial Canary Current; NADC, North Atlantic Drift Current; NSG, Nova Scotia Current; LC, Labrador Current; CNAG, Central North Atlantic Gyre; NEAC, Northeast Atlantic Current; RC, Reykjaenes Current; EGC, East Greenland Current; WGC, West Greenland Current; and SIC, South Iceland Current.

of which were controlled by the rapid oscillations in the Arctic-Greenland ice cap. Mediterranean pollen and African dust records, on the other hand, suggest a link between Mediterranean continental aridity and dust transport from the African continent and thus a low-latitude climate connection [*Cacho et al.*, 2000, 2001; *Combourieu-Nebout et al.*, 2002; *Sanchez-Goñi et al.*, 2002; *Moreno et al.*, 2004].

[4] Within marine oxygen isotope stage 100 (MIS100; ~2.52 Ma), rapid changes occurred in Mediterranean SST, THC and African dust supply to the central Mediterranean Monte San Nicola (SN) section (Sicily, Italy) and eastern Mediterranean Ocean Drilling Program (ODP) Site 967, implying a common climatic forcing mechanism [*Becker et al.*, 2005]. Specifically, rapid fluctuations in foraminiferal $\delta^{18}O$ values and abundance pattern of the cold-water planktonic foraminiferal species, *Neogloboquadrina atlantica*, i.e., precursor of left coiling *N. pachyderma*, are similar in temporal spacing to those reflected in late Pleistocene western Mediterranean sediments. This suggests that D-O and H-like climate variations also characterized by millennial to sub-Milankovitch-scale changes in the Mediterranean during MIS100.

[5] In order to assess the climate link between the Mediterranean and the North Atlantic during late Pliocene MIS100 and to test whether the fast climate variations observed in Mediterranean SST and THC coincide with similar SST changes and ice rafting episodes in the North Atlantic, we constructed new high-resolution proxy data (*N. atlantica* percentages, lithic counts and benthic stable isotopes) from North Atlantic ODP Site 981 and Deep Sea Drilling Project (DSDP) Site 607 located at the northern and southern boundary of the ice rafting belt [*Ruddiman et al.*, 1989]. For a common age scale the Mediterranean astronomically calibrated age scale [*Becker et al.*, 2005] was exported to the Atlantic by means of benthic oxygen isotope stratigraphy. Our study reveals that SST changes in the Mediterranean varied in conjunction with episodes of major (spacing of 3–4 kyr) and minor (spacing of 1.5–2 kyr) ice-rafted debris (IRD) events in the North Atlantic during MIS100, which culminated in a stadial-interstadial alternation of 6–8 kyr. We suggest that the underlying climatic mechanisms are similar to the D-O and H event type of changes that influenced the Mediterranean during the late Pleistocene [e.g., *Cacho et al.*, 1999] despite the much smaller ice sheets during the Pliocene. We will further suggest that changes in Mediterranean and Atlantic SST and THC observed on the longer stadial-interstadial timescale (6–8 kyr) are probably driven by low-latitude processes, with the role of orbital precession to be evaluated in further studies.

2. Materials and Methods

[6] DSDP Leg 94 Site 607 (32°58′W 41°00′N) is situated on the western flank of the Mid-Atlantic Ridge at a depth of 3427 m. Surface waters are influenced by the North Atlantic Drift on the northern limb of the subtropical gyre (Figure 1).

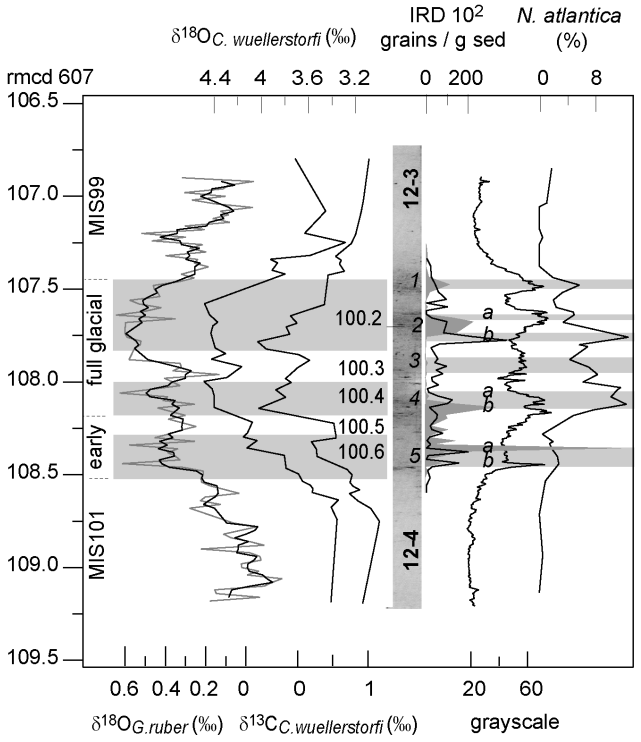

Figure 2. Planktonic and benthic oxygen isotope data and benthic carbon isotope data of DSDP Site 607 plotted versus revised meter composite depth (rmcd) (labeled a). Note that $\delta^{18}O$ curves are plotted inversely. The $\delta^{18}O_{G.ruber}$ curve (shaded line) is overlain by a three-point moving average (dark line). Stadial and interstadial phases within MIS100 are shaded and labeled by even numbers with early and full glacial phases being indicated on the left hand axis. Black and white core photograph of cores 12-3 (7–150 cm) and 12-4, dark (dark line) and light (shaded line) lithic particle counts, gray-scale measurements and *Neogloboquadrina atlantica* percentages are shown. Intervals with high amount of ice-rafted debris (IRD) are shaded and labeled 1–5.

During past glacial stages, this site was positioned at the southern margin of the IRD belt [*Ruddiman et al.*, 1989] and was a sensitive recorder of both circum-North Atlantic ice sheet extent and variability in meridional heat transfer from the equatorial region [*Ruddiman et al.*, 1986]. Today, bottom water at this site is composed predominantly of North Atlantic Deep Water (NADW), whereas during glacial periods of the late Pliocene and Pleistocene benthic foraminiferal $\delta^{13}C$ values indicate the presence of a low $\delta^{13}C$ water mass, probably southern ocean water (SOW) [*Raymo et al.*, 1989, 2004].

[7] ODP Leg 162 Site 981 (55°28′N, 14°39′W) is located east of the Rockall Bank at a depth of 2173 m. At present, deep water at this site is a combination of lower NADW, recirculated from the southern part of the North Atlantic, and a small component of water overflowing the Wyville-Thompson Ridge (Wyville-Thompson Ridge Overflow Water; WTRO) [*Schmitz and McCartney*, 1993]. Similar to Site 607, benthic foraminiferal $\delta^{13}C$ values indicate the presence of a low $\delta^{13}C$ water mass during glacial periods.

[8] MIS95-101 were originally defined at Site 607 [*Raymo et al.*, 1989] and can be easily recognized in Site 981 based on paleomagnetic, calcareous nannofossil and planktonic foraminiferal datums [*Channell and Lehman*, 1999; *Flower*, 1999]. MIS100 appears as a dark interval in the cores and is characterized by distinct short-term color changes (Figures 2 and 3). MIS100 of Site 607 was sampled in a continuous interval of core sections 607-12H-3-71 cm to 12H-4-149 cm (106.90–109.18 rmcd) with 10 cc samples being taken every 2 cm. Dry bulk density was calculated by weighing samples before and after drying at 50°C. Subsamples for stable isotope measurements and lithic compounds counting were taken from the dried samples. Samples were washed through 37, 63, 125 and 600 μm meshes of which each fraction was weighed.

[9] MIS100 of Site 981 was sampled following the composite depth profile (Scientific Shipboard Party [*Jansen et al.*, 1996a, 1996b]) every 5 cm in the interval 981C-17H-4-46 cm to 17H-5-115 cm and 981B-18H-3-52 cm to 135 cm (169.94–174.53 mcd) with an overlap of 30 cm between Hole C and B. Samples were freeze-dried, washed through 63, 150 and 600 μm meshes and the residual of each fraction be weighed.

[10] The planktonic foraminiferal stable isotope measurements of Site 607 were carried out on about 30 specimens of the species *Globigerinoides ruber* (white) that were handpicked from a split of the >212 μm size fraction. The analysis was carried out at the Department of Earth Sciences

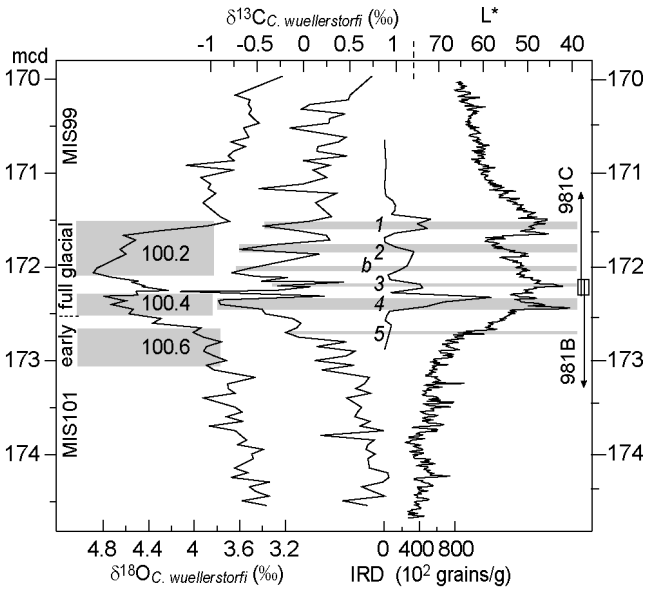

Figure 3. Benthic oxygen, carbon isotope, IRD, and color reflectance (L*) data of ODP Site 981 plotted versus meter composite depth (mcd). Note that L* and $\delta^{18}O$ are plotted inversely. Here $\delta^{18}O$ is plotted on the same scale as in Figure 2. The early and full glacial phases are indicated on the left hand axis; shaded areas and labels indicate stadials and intervals of low $\delta^{13}C_{benthos}$. The overlap between Holes C and B of Site 981 is indicated on the right axis.

(Utrecht University), where an ISOCARB common bath carbonate preparation device is linked to a VG SIRA24 mass spectrometer. Isotope values were calibrated to the Peedee belemnite (PDB) scale using an in-house carbonate standard (NAXOS). Analytical precision was determined by replicate analyses and by comparison to the international IAEA-CO1 and NBS19 standard. Replicate analyses showed standard deviations of ±0.06‰ and ±0.1‰ for $\delta^{13}C$ and $\delta^{18}O$, respectively.

[11] The benthic foraminiferal stable isotope analyses of Sites 607 and 981 were carried out on 2–4 specimens of the species *Cibicidoides wuellerstorfi*, hand-picked from the >212 μm fraction. Stable isotope measurements were done at the faculty of Earth and Life Sciences (Amsterdam Free University) where a CARBO-KIEL automated carbonate preparation device is linked to a FINNIGAN MAT252 mass spectrometer. Replicate analysis and calibration to the international carbonate standard NBS19 and in-house standard revealed analytical precision better than ±0.05‰ and ±0.1‰ for $\delta^{13}C$ and $\delta^{18}O$, respectively. *Cibicidoides wuellerstorfi* oxygen isotope values have been adjusted by +0.64‰ in order to be in equilibrium with ambient seawater [*Shackleton and Opdyke*, 1976; *Shackleton and Hall*, 1984].

[12] Lithic grains were counted in the fraction 125–600 μm and 150–600 μm of Sites 607 and 981, respectively. Dark and light particles at Site 607 were counted separately; the "dark" particles include sharp-edged rock fragments, single mineral grains and transparent rounded quartz grains. The "light" grains are soft carbonate agglomerates containing occasional foraminifera. Lithic particles at Site 981 include sharp-edged rock fragments, single mineral grains, transparent quartz grains and traces of carbonates, hematite-coated grains and volcanic components.

[13] Gray-scale measurements were carried out on digital scans of the Site 607 black and white core photographs using the Scion Image 4.0 freeware image analysis software. Artificial color changes related to small cracks in the sediment and other disturbances were manually removed from the color profile. The color reflectance of Site 981 was measured at Bremen core repository on the archive half of core 981C-17H-4-46 cm to 17H-5-115 cm and 981B-18H-3-52 cm to 135 cm (169.94–174.53 mcd) every centimeter following the composite depth profile (Scientific Shipboard Party [*Jansen et al.*, 1996a, 1996b]) using a hand-held Minolta CM 503i spectrophotometer.

[14] Lastly, foraminifers were counted at Site 607 in the interval between 12H-3-87 cm and 12H-4-85 cm (107.06–108.54 rmcd) with samples every 4 cm on average (32 samples in total). Faunal samples were split using an "Otto microsplitter" until a total number of 200 to 300 planktonic foraminifers per sample was obtained. Only the temperature-sensitive species *Neogloboquadrina atlantica* (s), *Neogloboquadrina pachyderma* (d) and *Globigerinoides ruber* (white) were counted with respect to the total number of foraminifers per split. *N. pachyderma* was distinguished from *N. atlantica* by the typical flat initial spiral of the oldest chambers and the usually thicker wall structure. Moreover, *N. pachyderma* is predominantly dextral coiled, while *N. atlantica* has an often extraumbilical aperture and is predominantly sinistral coiled (~95%).

3. Results

3.1. Stable Isotopes

[15] The oxygen isotope values of *Cibicidoides wuellerstorfi* ($\delta^{18}O_{benthos}$) at Site 607 vary from ~3.3‰ during MIS99 and MIS101 to maximum values of ~4.5‰ during MIS100, implying a glacial-interglacial (G-I) difference of ~1.2‰ (Figure 2). Three stadial intervals can be distinguished within MIS100 and were labeled MIS100.6, MIS100.4 and MIS100.2 following the Mediterranean benthic isotope chronology of this stage [*Becker et al.*, 2005]. Evidently, MIS100.6 is only reflected by a small bulge in the MIS101/100 transition, whereas stadials MIS100.4 and MIS100.2 reflect full glacial conditions. During interstadial MIS100.3, $\delta^{18}O_{benthos}$ values decrease from a full glacial value of ~4.5‰ to ~4.2‰. At Site 981, interglacial (~3.4‰) and glacial (~4.8‰) $\delta^{18}O_{benthos}$ values are slightly heavier by ~0.2‰ and ~0.4‰ than at Site 607 (Figure 3), resulting in a G-I difference of ~1.4‰. MIS100.4 and MIS100.2 are clearly defined in Site 981. The intervening interstadial MIS100.3 is marked by a severe drop in $\delta^{18}O_{benthos}$ values of up to 0.6‰ (from ~4.8‰ to ~4.2‰).

[16] The planktonic oxygen isotope ($\delta^{18}O_{G.ruber}$) values of Site 607 are ~0‰ in the interglacial and ~0.6‰ in the glacial (Figure 2). Superimposed on the long-term glacial-interglacial change, oxygen isotope values fluctuate by ~0.4‰, indicating short-term changes in $\delta^{18}O$ of ambient water within both the glacial and interglacial periods.

[17] The benthic carbon isotope record ($\delta^{13}C_{benthos}$) of Site 607 depicts a negative correlation to the $\delta^{18}O_{benthos}$. Interglacial $\delta^{13}C_{benthos}$ values average 1‰, while glacial values vary between −0.5 and 0.5‰. Lowest $\delta^{13}C_{benthos}$ values occur during the three stadial periods (Figure 2). The $\delta^{13}C_{benthos}$ values of Site 981 are on average 0.2‰ more negative than at Site 607 (Figure 3), being ~0.8‰ in the interglacial and between −0.75 and 0.4‰ in the glacial. The $\delta^{13}C_{benthos}$ record of Site 981 shows more frequent and higher amplitude variability during the studied interval than that of Site 607. Note that Site 981 contains only four more data points than Site 607 within MIS100 (i.e., ~31 versus 27). Clearly, at least five episodes with negative $\delta^{13}C$ excursions occur during MIS100: one at the base of MIS100, one in MIS100.4, one in MIS100.3, and two within MIS100.2. Additional depletions occur at the MIS100/MIS99 and MIS101/MIS100 transitions. The smaller fluctuations in $\delta^{13}C_{benthos}$ during MIS100.3 are related to small differences in $\delta^{13}C_{benthos}$ values between samples from Hole C and B of Site 981.

3.2. Color Reflectance, Lithic Grain and Faunal Counts

[18] The gray-scale record of Site 607 shows five intervals (1–5) in MIS100 that exhibit a darker sedimentary color (Figure 2). These dark-colored intervals contain high concentrations of lithic particles >150 μm. Comparison of dark (black line) and light (grey shaded) particle numbers with the gray-scale record reveals that both signals contribute to the lightness variations, although they do not peak

simultaneously. One distinctive dark lithic particle abundance increase occurs below the second youngest dark layer, which is not reflected in the gray scale (labeled as 2b). We interpreted the darker layers and associated enhanced lithic components at Site 607 as representing the episodic input of IRD. It is however not ambiguous whether the light-colored fragments are also IRD, because the softness and agglomeration character as well as the inclusion of small foraminifers may indicate that these particles are either a product of biological (fecal) pellets or of in situ calcium carbonate dissolution. In particular, high numbers of light-colored particles correlate with the most severe $\delta^{13}C$ depletions, which may indicate carbonate dissolution due to the presence of more corrosive bottom waters. The foraminiferal tests, however, do not show any sign of carbonate dissolution, which could indicate that the light-colored particles are the result of the agglomeration of fine carbonate particles by burrowing organisms.

[19] Concentrating on the dark lithic group, which is clearly related to IRD, reveals that the darker intervals of in particular events 5, 4 and 2 consist of multiple ice rafting episodes (Figure 2). This interpretation is strengthened by the peak occurrences of *Neogloboquadrina atlantica*, coincident with these five main and three minor IRD events. *N. atlantica* is an extinct species that was endemic to high-latitude North Atlantic cold surface water environments during late Miocene to Pliocene [*Poore and Berggren*, 1975; *Raymo et al.*, 1986; *Meggers and Baumann*, 1997]. Biometric data shows that in the North Atlantic *N. atlantica* adapted selectively to the global late Neogene cooling and therefore was suggested to be temperature-sensitive [*Meggers and Baumann*, 1997]. Although *N. atlantica* was classified as a subpolar species it might represent a cold water end-member for the late Pliocene similar to its modern relative *Neogloboquadrina pachyderma* (sinistral) [*Raymo et al.*, 1986; *Meggers and Baumann*, 1997].

[20] Similar, dark IRD-rich horizons at Site 981 coincide with the six episodes of low $\delta^{13}C_{benthos}$ values (Figure 3). The second and third youngest depletion in $\delta^{13}C_{benthos}$ are characterized by one single IRD event, probably because of the poor sample resolution (15 cm) in this interval. In addition, the IRD variability at Site 981 seems less frequent than at Site 607, which is due to the lower resolution of lithic counts at Site 981 (half that of Site 607).

3.3. Correlation Between Atlantic and Mediterranean

[21] For the studied interval of Sites 981 and 607 a timescale was constructed using the visual correlation between $\delta^{18}O_{benthos}$ records of both sites and that of the Mediterranean SN section. This resulted in an astronomically tuned age model for all sites, since SN was tied to Site 967. The age model of this latter site was based on the tuning of its Ti/Al record to the 65°N summer insolation curve of the $La04_{(1,1)}$ astronomical solution [*Lourens et al.*, 2001; *Becker et al.*, 2005]. Six tie points were set to calibrate Site 607 to the $\delta^{18}O_{benthos}$ of SN (Figure 4): one at each glacial-interglacial transition, one within MIS100.3, one just above MIS100.0 and two, which tie the $\delta^{18}O_{G.ruber}$ record of Site 607 to the $\delta^{18}O_{G.ruber}$ of SN. Linear interpolation was applied between the age points resulting in average sedimentation rates of 4.7 cm/kyr in MIS99, 6 cm/kyr in MIS100 and 3.4 cm/kyr in MIS101.

[22] Only four tie points were used to correlate Site 981 to SN: one at each glacial-interglacial transition, one in MIS100.4 and one in MIS100.3. This results in an average sedimentation rate of 8.7 cm/kyr during MIS100. Ages for interglacial MIS99 and MIS101 were calculated assuming average sedimentation rates of 13.7 cm/kyr and 17.3 cm/kyr, respectively. These sedimentation rates were achieved by comparing our high-resolution $\delta^{18}O_{benthos}$ data of Site 981 with the lower-resolution $\delta^{18}O_{benthos}$ data of *Draut et al.* [2003] (MIS104-95) from the same site and tying minimum $\delta^{18}O_{benthos}$ during MIS101 and MIS99 to minimum $\delta^{18}O_{benthos}$ values of Site 967 during these interglacial periods, respectively.

[23] The Mediterranean and Atlantic benthic oxygen isotope records display the typical asymmetric structure of a slow glacial buildup and a rapid termination (Figure 4) that was also observed for other late Pliocene and Pleistocene glacial cycles [*Raymo*, 1992]. Small offsets in the $\delta^{18}O_{benthos}$ values between the various sites probably indicate differences in ambient bottom water isotopic composition ($\delta^{18}O_w$) with SN being the warmest and shallowest site. The MIS100/MIS99 transition corresponds with a sharp decrease in $\delta^{18}O_{benthos}$ of 0.8‰ in all four records. The well defined MIS100.3 (interstadial phase) and MIS100.4 and MIS100.2 (stadial phases) of SN are clearly expressed in Sites 607 and 981, but not in Site 967, while MIS100.6 and MIS100.5 are not well expressed in the $\delta^{18}O_{benthos}$ records of either the Atlantic or Site 967. The timescale reveals that each stadial-interstadial couplet had durations of 6–8 kyr (Figure 4).

[24] The $\delta^{18}O_{G.ruber}$ records of Site 607, Site 967 and SN show very similar patterns (Figure 4). Stadial and interstadial phases as defined in the Mediterranean $\delta^{18}O$ record are clearly reflected in the $\delta^{18}O_{G.ruber}$ record of Site 607, although the amplitude of changes at Site 607 are half of that in the Mediterranean records. This difference may be due to the low temperature tolerance (14°–32°C) of *G. ruber* [*Schmidt and Mulitza*, 2002]. The overall low relative abundance (0–1%) of *G. ruber* at Site 607 during glacial stage 100 indicates that (summer) SST were probably around the lower tolerance temperature of this species and slightly higher during interstadials. Consequently, the $\delta^{18}O_{G.ruber}$ record of Site 607 might reflect only the warmest summers during MIS100 and thus be biased toward warmer summer temperatures.

[25] The relative abundance pattern of *N. atlantica* at Site 607 and SN are generally similar, showing highest abundances during IRD peaks and $\delta^{13}C_{benthos}$ minima in both North Atlantic sites (Figure 5). Although *N. atlantica* was counted at lower resolution in Site 607, major *N. atlantica* peaks (1–5 including multiple peaks during 4a and 4b and 2a and 2b) are reflected in both records. The spacing of events is on the order of 3–4 kyr for major events 1–5 and approximately 1.5–2 kyr for the less distinct events 5a, 5b, 4a, 4b and 2a and 2b. Remarkably, during MIS100.3, *N. atlantica* reached highest percentages in the Mediterranean, whereas the most depleted $\delta^{13}C_{benthos}$ values were recorded at Site 981. Moreover this interval corresponds with

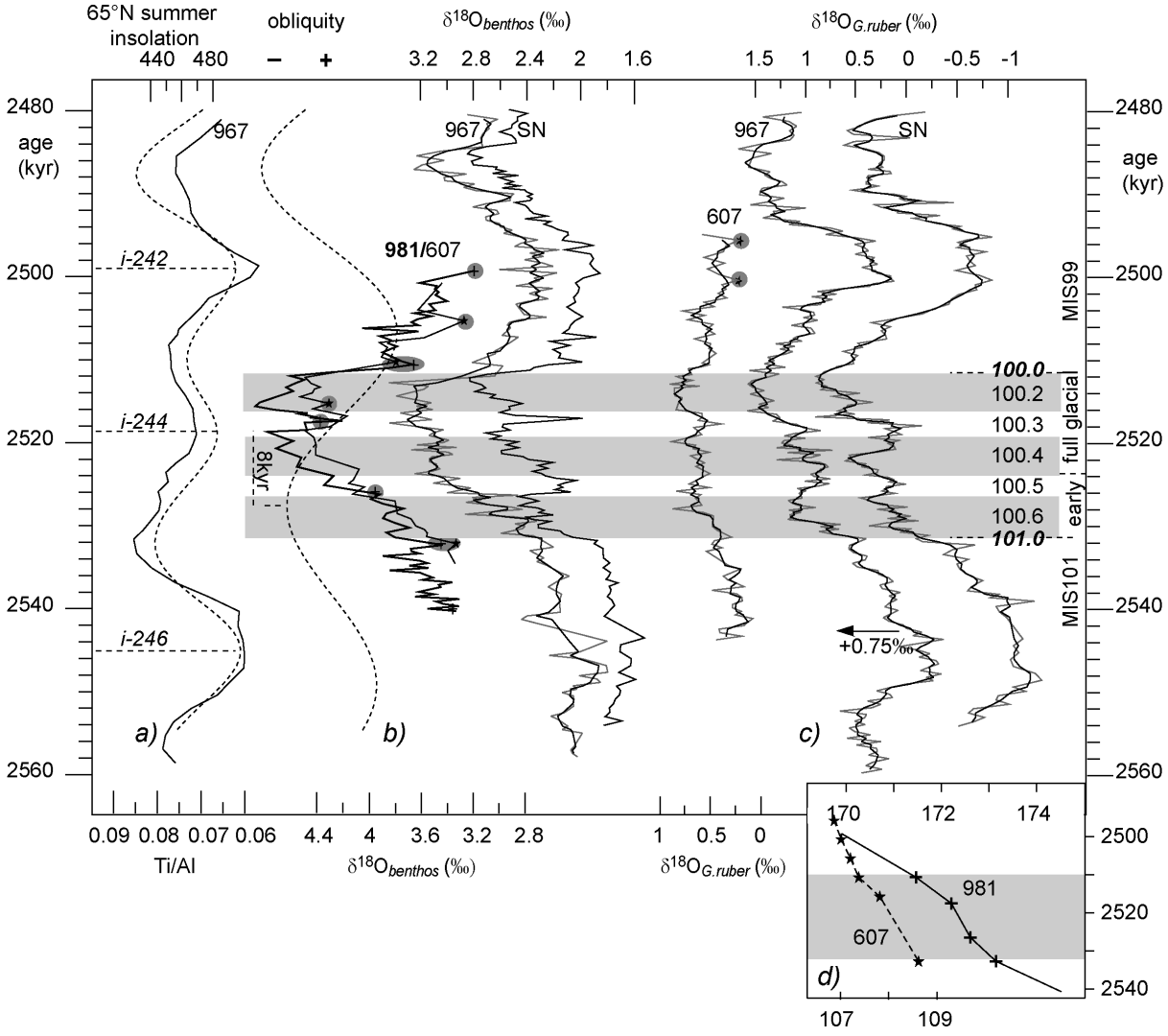

Figure 4. Age calibration of DSDP Site 607 and ODP Site 981 to Mediterranean ODP Site 967A and San Nicola (SN) land section. (a) Ti/Al of Site 967A (inversed axis, data from *Lourens et al.* [2001]) and $La04_{(1,1)}$ 65°N summer insolation (dashed line). The i cycles on the left age axis indicate numbering of insolation maxima according to *Lourens et al.* [1996]. (b) The $\delta^{18}O_{benthos}$ of Sites 981 (thick line), 607, and 967A (shaded line overlain by three-point moving average) and SN in relation to $La04_{(1,1)}$ obliquity (dashed line). All $\delta^{18}O_{benthos}$ data are plotted on the same scale (inverse axis). Stars (Site 607) and crosses (Site 981) indicate age calibration points. (c) The $\delta^{18}O_{G.ruber}$ of Sites 607 and 967 and SN each overlain by a three-point moving average. Notice that the $\delta^{18}O_{G.ruber}$ of Site 967 has been shifted by 0.75‰ toward heavier values for clarity. Shaded areas and even labels indicate stadials according to *Becker et al.* [2005]. The early and late glacial are indicated on the left age axis. (d) Age-depth (kyr-mcd) relation for Sites 607 (stars) and 981 (crosses). Ages are linearly interpolated between calibration points. The shaded interval indicates MIS100.

a less marked IRD event at Site 607 accompanied by the temporal occurrence of *Globorotalia menardii* (Figure 5).

4. Discussion

[26] Millennial-scale changes in IRD abundance, *N. atlantica* percentages and $\delta^{13}C_{benthos}$ values within MIS100 indicate that North Atlantic climate was not stable, but underwent brief reorganizations in SST, ice distribution and THC. The 1.5- to 4-kyr spacing between these rapid changes is very similar in nature and duration to that of the Pleistocene D-O cycles. Peak abundance of *N. atlantica* at Site 607 during MIS100 are therefore considered to reflect similar climatic conditions as those of *N. pachyderma* (s) during the early and late Pleistocene, which have been unambiguously correlated to the cold phase of the D-O oscillations and H events [*Bond*, 1992; *Bond et al.*, 1993; *Raymo et al.*, 1998; *Bond et al.*, 1999]. In addition, the

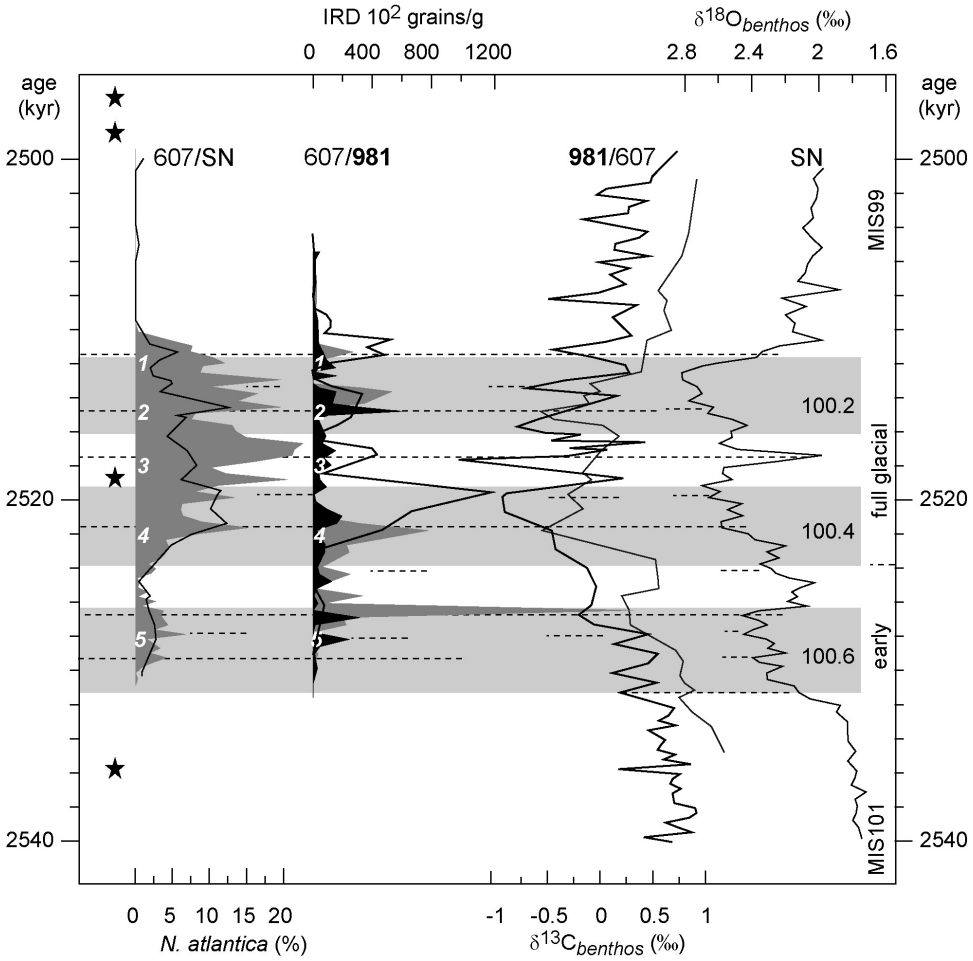

Figure 5. *N. atlantica* percentages of Site 607 (solid line) and SN (shaded), IRD of Site 607 (dark particles are shaded dark gray, light particles are shaded light gray) and Site 981 (thick line), $\delta^{13}C_{benthos}$ Site 981 (thick line) and Site 607 (thin line), and $\delta^{18}O_{benthos}$ of San Nicola versus age (kyr). Note that the IRD record of Site 607 is stretched by a factor 2 to match the IRD record of Site 981. Dashed lines and numbers indicate spacing of the events. Shaded areas and even labels indicate stadials. Early and full glacial periods are indicated on the left age axis. Stars near the left axis indicate the occurrence of *Globorotalia menardii*.

concomitant peak occurrences of *N. atlantica* in both SN and Site 607 indicate that Mediterranean surface waters varied on the same D-O scale. This resembles the pattern of the late Pleistocene, where peak abundances of *N. pachyderma* (s) in the western Mediterranean are related to the cold phases of the D-O cycles and H events [*Rohling et al.*, 1998; *Cacho et al.*, 2000].

[27] The stadial-interstadial $\delta^{18}O_{benthos}$ changes during MIS100 indicate furthermore that the climate conditions in the Mediterranean and adjacent Atlantic have changed on timescales in between the D-O and Milankovitch periods (i.e., on the order of 6–8 kyr). The mechanism causing this regular alternation of stronger and weaker glacial conditions seems to have affected SST and/or sea surface salinity (SSS) conditions at Site 607 during interglacial periods as well with approximately the same rate of recurrence, as evidenced by changes in the $\delta^{18}O_{G.ruber}$ record of this site. Stadial-interstadial alternations in the $\delta^{18}O_{benthos}$ of SN were shown to vary in parallel to SST changes with slow cooling during stadials followed by abrupt warming at the stadial/interstadial boundary [*Becker et al.*, 2005]. Hence the correlation between these abrupt warming events in the SN record and the major IRD events 1, 3 and 5 in the North Atlantic in combination with an average spacing of these events of 6–8 kyr strongly suggests that these stadial-interstadial alternations represent climate changes comparable to the so-called late Pleistocene Bond cycles. Accordingly, the IRD events 1, 3 and 5, related to the terminal phases of these cycles, would be equivalent to the Heinrich events.

4.1. North Atlantic–Mediterranean Climate Linkages

[28] Today, the relatively warm water masses of the North Atlantic Current (NAC) and the North Atlantic Drift Current (NADC) (Figure 1a) are responsible for the mild climate in Europe by bringing warm moist air across the European

continent [*Otterman et al.*, 2002]. This mechanism was probably activated by the initiation of the Labrador Current during the Middle Pliocene [*Spaak*, 1983]. Since this time changes in the position of the NADC may have caused significant latitudinal alteration in the climate zones of Western Europe on all timescales [*Otterman et al.*, 2002]. During the last glacial maximum (LGM), the frontal systems were displaced southward in the presence of glaciers and sea ice, leading to a North Atlantic surface circulation pattern. This consisted of two main gyre systems (Figure 1b, redrawn after *Robinson et al.* [1995]): the warm, sluggish Central North Atlantic Gyre (CNAG) north of ~40°N and the Glacial Subtropical Gyre (GSG) south of ~40°N [*Robinson et al.*, 1995; *Seidov and Maslin*, 1999]. This configuration resulted in large-scale cooling of the European continent [*Sarnthein et al.*, 1995; *Cortijo et al.*, 1997], delivery of IRD to the Gulf of Cadiz [*Bard et al.*, 2000], inflow of cold Atlantic surface water into the Mediterranean [*Asioli et al.*, 1999; *Cacho et al.*, 1999] and D-O-related SST and THC changes in the Alboran and Ligurian Seas [*Rohling et al.*, 1998; *Cacho et al.*, 2000, 2001; *Combourieu-Nebout et al.*, 2002].

[29] It has been well documented that Mediterranean SST conditions varied in phase with the obliquity-controlled global ice volume changes and North Atlantic climate throughout the late Pliocene and early Pleistocene [*Zachariasse et al.*, 1990; *Lourens et al.*, 1992; *Versteegh*, 1997]. The strongest evidence is given by the synchronous occurrence of *N. atlantica* and *Neogloboquadrina pachyderma* (s) in the Mediterranean and the Atlantic Site 607 during glacial stages 110–96 and 64–34, respectively [*Zachariasse et al.*, 1990; *Lourens et al.*, 1992]. The appearance of these species in the Mediterranean was linked to the inflow of cold (high latitude) Atlantic surface waters through the Strait of Gibraltar [*Spaak*, 1983]. Pollen data further indicate that with the extension of glaciers and sea ice in the Northern Hemisphere, polar air masses expanded southward and cooled the European continent during MIS100 [*Willis et al.*, 1999] and subsequent glacial stages [*Combourieu-Nebout*, 1991]. A more southerly position of the polar front during MIS100 is also evidenced by perennial sea ice cover in the Norwegian Greenland Sea (NGS) [*Henrich et al.*, 2002].

[30] The synchrony between peak occurrences of *N. atlantica* in the Mediterranean and adjacent North Atlantic suggests that short-term recurrent pulses on millennial timescales were superimposed upon the southward extension of Atlantic polar waters during MIS100. In addition to the direct inflow of colder Atlantic surface waters, a strengthening and northward displacement of the northwesterlies may have favored prolonged winter anticyclone stability over central and northern Europe. This would have resulted in a strong southward flow over the Mediterranean region and very cold and dry Mediterranean winters [*Cacho et al.*, 2000, 2001; *Combourieu-Nebout et al.*, 2002; *Sanchez-Goñi et al.*, 2002; *Moreno et al.*, 2004]. The inferred cold air outbreaks from the European continent during winter should have enhanced surface water cooling and vertical convection and facilitated the peak occurrences of *N. atlantica* and the cold water benthic species *Cibicides cf. ungerianus* and *Trifarina angulosa* at SN [*Becker et al.*, 2005].

[31] A comparison between the abundance patterns of *N. atlantica* and IRD, and the northern African dust signal recorded by the bulk sediment composition of SN and Ti/Al record at ODP Site 969 in the central Mediterranean [*Becker et al.*, 2005] reveals that the cold episodes of the D-O-like cycles in the North Atlantic and Mediterranean coincide with enhanced dust supply from the African continent to the central Mediterranean (low $CaCO_3$ wt% and high Ti/Al values, Figure 6). This suggests that during these episodes northern African climate was much drier and/or that the storm tracks responsible for the dust supply were intensified. Hematite contents derived from magnetic properties at Site 967 indicate increased aeolian dust supply to the eastern Mediterranean related to low monsoon intensities during the minimum in the 400 kyr eccentricity ~2.5–2.4 Ma [*Larrasoaña et al.*, 2003]. Although this 3 Ma record suggest that higher-frequency fluctuations (i.e., <15 kyr) in aeolian dust supply become significant above ~0.95 Ma, our MIS100 data is in accordance with the late Pleistocene dust record from the Alboran Sea, that shows that intervals of high dust delivery from the African continent into the western Mediterranean are contemporary to the high dust fluxes during the cold D-O episodes of the Greenland ice cores [*Moreno et al.*, 2002]. *Moreno et al.* [2002] proposed that the pronounced equatorward expansion of the polar regime during cold D-O and H episodes would have reduced the transfer of heat to the high latitudes, increased the meridional temperature gradient and hence affected the latitudinal trajectory of westerlies crossing the North Atlantic. As a result, channeling of the storm pathways further to the south and strengthening of the high-pressure cell above the subtropical Atlantic may have caused an increase in the dust transport from the Saharan desert to the Mediterranean [*Moreno et al.*, 2002].

4.2. Changes in Thermohaline Circulation

[32] The waxing and waning of the Northern Hemisphere ice sheets could largely explain the strong climate linkages between the North Atlantic and Mediterranean on Milankovitch (obliquity), stadial-interstadial (H, 6–8 kyr), and millennial (D-O) timescales of MIS100. For instance, the 0.3–0.6‰ drop during MIS100.3 could indicate that besides local changes in temperature and/or salinity a significant change in global ice volume may have occurred. Moreover, the asymmetric $\delta^{18}O_{benthos}$ pattern associated with MIS100.3 is in good agreement with a fast waning and slower waxing of ice masses as predicted by ice sheet models [*MacAyeal*, 1993]. The amplitude of the $\delta^{18}O_{benthos}$ change during MIS100.3, however, is one third to one half the magnitude of the assumed $\delta^{18}O_{benthos}$ G-I variation during MIS100, which would imply melting of large parts of the land-based ice sheets within a few hundred years if this variability is attributed to ice volume changes alone.

[33] Changes in ice sheet volume were probably not the only mechanism causing the stadial-interstadial variability in the $\delta^{18}O_{benthos}$ records, since the $\delta^{18}O_{G.ruber}$ record of Site 607 also reflects pervasive variability during MIS99 and MIS101 with similar amplitude and spacing as during

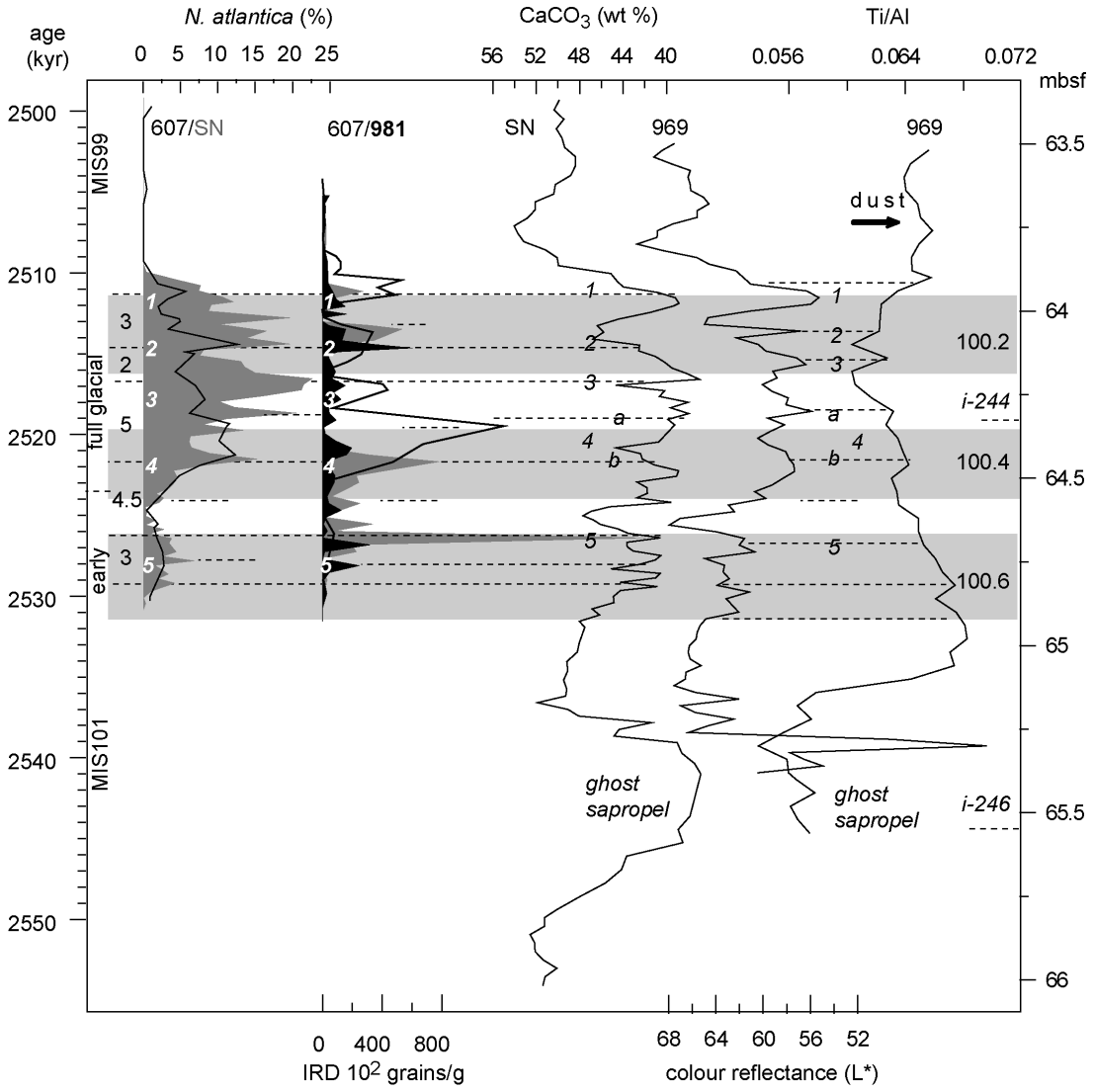

Figure 6. *N. atlantica* percentages of Site 607 (solid line) and SN (shaded), IRD of Sites 981 (thick line) and 607 (dark particles are shaded dark gray, light particles are shaded light gray), and $CaCO_3$ weight percentages of SN versus age (kyr). Note that the IRD record of Site 607 is stretched by a factor 2 to match the IRD record of Site 981. Italic numbers label IRD events 1–5. Dashed lines and numbers on the left axis indicate the spacing of IRD events. Further labeling is according to Figure 4. Color reflectance (L*) and Ti/Al of Site 969 (data from *Wehausen* [1999]) versus meters below seafloor (mbsf) are shown. Dashed lines and italic numbers indicate IRD events 1–5 and related $CaCO_3$ minima in SN. High Ti/Al values indicate high amounts of African dust [*Becker et al.*, 2005].

MIS100. This may imply that changes in SST and sea surface salinity (SSS) could have played a crucial role in changing the deep water composition in the North Atlantic during full glacial conditions, most likely through changes in the THC. Such a scenario is in agreement with the stadial-interstadial variability reflected in the $\delta^{13}C_{benthos}$ record of Site 607. Low glacial $\delta^{13}C_{benthos}$ values of deep North Atlantic records are commonly interpreted as reflecting the increased influence of Southern Ocean Water (SOW), which is depleted in ^{13}C relative to NADW [*Raymo et al.*, 2004; *Curry and Oppo*, 2005; *Robinson et al.*, 2005]. The $\delta^{13}C_{benthos}$ values of Site 607 during MIS100 lie on the glacial mixing line [*Raymo et al.*, 1990, 1992] between $\delta^{13}C_{benthos}$ values from the Pacific (Sites 846, 849 and V28-179), equatorial Atlantic (Site 659) and North Atlantic (Sites 552 and 610), indicating increased influence of SOW and suppression of NADW at this site (Figure 7, see Table 1 for site information). Consequently, the relatively high $\delta^{13}C_{benthos}$ values (0.25‰) during MIS100.3 at Site 607 would indicate a short interval of enhanced NADW production and hence stadial-interstadial variations in THC. Additional evidence for stadial-interstadial changes in THC may come from the $\delta^{13}C_{benthos}$ record of ODP Site 658 (off northwest Africa) where despite

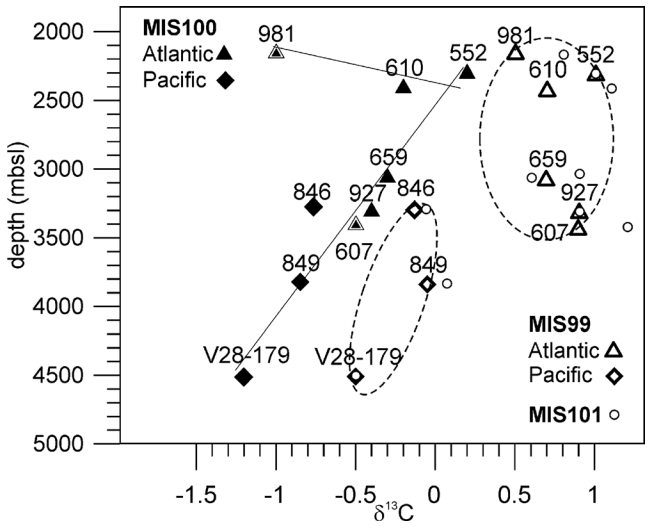

Figure 7. The $\delta^{13}C_{benthos}$ data of MIS100 (solid symbols) and MIS99 (open symbols) from different Pacific (diamonds) and North Atlantic (triangles) cores (see labels, for core location and reference see Table 1) versus depth (meters below sea level). Dashed circles indicate Atlantic and Pacific origins for interglacial $\delta^{13}C_{benthos}$ values. The $\delta^{13}C_{benthos}$ values of MIS101 (open circles not labeled) match $\delta^{13}C_{benthos}$ values during MIS99. Glacial (MIS100) $\delta^{13}C_{benthos}$ values lie on a mixing line between $\delta^{13}C_{benthos}$ values of the Pacific and North Atlantic Site 522. On the contrary, glacial $\delta^{13}C_{benthos}$ values of Site 981 lie off the mixing line.

low sample resolution a prominent (~0.6‰) increase in the $\delta^{13}C_{benthos}$ record is recorded approximately halfway through MIS100 [*Tiedemann*, 1991]. This $\delta^{13}C_{benthos}$ increase points toward a short interval of enhanced THC within MIS100, which is probably equivalent to the one observed during MIS100.3 at Site 607.

[34] In contrast to Site 607, MIS100.3 at Site 981 is characterized by the lowest $\delta^{13}C_{benthos}$ values of MIS100 and by high abundances of IRD. This remarkable difference between Sites 981 and 607 could be explained by the more complex oceanographic position of Site 981 and the different timescales on which the $\delta^{13}C_{benthos}$ records of these sites were fluctuating: That is, the $\delta^{13}C_{benthos}$ record at Site 607 primarily changed on stadial-interstadial timescales during MIS100, whereas that of Site 981 is dominated by a D-O type of climate variability. The $\delta^{13}C_{benthos}$ values at Site 981 during MIS100 are more negative than those of Site 607 and are closer to Pacific $\delta^{13}C_{benthos}$ values, although fall off the Pacific-Atlantic mixing line (Figure 7). Therefore it seems unlikely that the low-$\delta^{13}C_{benthos}$ signature at Site 981 originates from SOW-mixing. Moreover, if SOW was the main water mass influencing Site 981 during MIS100, the $\delta^{13}C_{benthos}$ signature at both sites should have fluctuated at a similar pace. Instead, the very negative $\delta^{13}C_{benthos}$ values at Site 981 suggest the contribution of a water mass depleted in ^{13}C, probably surface water, which owes its low-$\delta^{13}C$ signature to a reduced sea-air exchange and/or suppressed surface water productivity during perennial sea ice cover in the NSG [*Raymo et al.*, 2004]. Such a low-$\delta^{13}C$ surface water signature could be exported to the deeper ocean by brine formation under sea ice, which has been considered the dominant mode of deep water formation in the NGS during the early Pleistocene [*Henrich and Baumann*, 1994] and the past few glacials [*Dokken and Jansen*, 1999; *Raymo et al.*, 2004]. Assuming, that such a process played a similar role during the late Pliocene, the very low $\delta^{13}C_{benthos}$ values at Site 981 during MIS100 indicated episodes of maximum influx of WTRO during periods of extensive sea ice formation in the NGS caused by cold phases of D-O type of climate conditions. This is in contrast to the slow stadial-interstadial changes observed in $\delta^{13}C_{benthos}$ of Site 607 and probably comparable with the observation from the LGM, that the intermediate ocean is decoupled from the global bipolar sea saw (THC) and instead associated in a more complex way with small climate changes above Greenland and the Arctic [*Robinson et al.*, 2005].

4.3. On the Origin of Sub-Milankovitch Climate Variability During MIS100

[35] A similar interfingering of climate signals at different pacing within MIS100 is also observed from the Mediterranean SN section. Within MIS100.3 short-lived peak occurrences of the benthic foraminifera *Trifarina angulosa* and *N. atlantica*, of which the latter reflects its highest abundance percentage of MIS100, were interpreted as reflecting strong winter mixing during extreme cold episodes of D-O type of climate variability. In contrast, lower Mediterranean SSS is evidenced from the planktonic $\delta^{18}O$ records of SN and Site 967 during the end of MIS100.4 and MIS100.3 and accompanied by increased relative abundances of *Neogloboquadrina* (dex.) at SN and enhanced Ba/Al values at Site 967. This may indicate enhanced primary productivity conditions [*Becker et al.*, 2005], a signature similar, although less amplified to that during sapropel formation in the Mediterranean during the late Pliocene [*Lourens et al.*, 1992; *Van Os et al.*, 1994]. The timing of MIS100.3 slightly lags a minimum in the astronomical precession index (insolation cycle i-244 [*Lourens et al.*, 1996]) by a few thousand years [*Becker et al.*, 2005] (see Figure 4)) but evidence is strong enough to state that the minimum in the precession index and associated maximum summer insolation at high northern latitudes may have set the stage for the origin of MIS100.3.

[36] Additional evidence that the precession cycle may have played a crucial role for triggering MIS100.3 comes from the temporal appearance record of *Globorotalia*

Table 1. Site Information

Site	Depth, mbsl[a]	Location	Data Reference
552	2301	56°N, 23°W	*Shackleton and Hall* [1984]
610	2417	53°N, 18°W	*Raymo et al.* [1992]
607	3427	41°N, 33°W	this study
846	3307	03°S, 91°W	*Shackleton et al.* [1995]
849	3851	00°N, 110°W	*Mix et al.* [1995]
927	3326	05°N, 44°W	*Bickert et al.* [1997]
981	2173	55°N, 15°W	this study
V28-179	4509	04°N, 139°W	*Shackleton and Opdyke* [1976]

[a]Meters below sea level.

menardii at Site 607 (Figure 5). This tropical-subtropical species [*Hilbrecht*, 1996] briefly occurred at Site 607 during MIS99, MIS101, and at the base of MIS100.3, matching closely with the positions of precession minima (taking into account the uncertainty in age calibration). *G. menardii* is an important marker species of the modern Azores Current (AC) [*Ottens*, 1991]. The presence of *G. menardii* at Site 607 therefore suggests short influxes of tropical-subtropical waters during MIS100.3. At the same time the high abundance of *N. atlantica* indicates cold (polar) water masses at Site 607 (and Mediterranean), again indicating two different climate signals present within MIS100.3. Assuming a LGM-like surface water circulation in the North Atlantic, Site 607 would be positioned on the boundary between the relatively cold waters of the CNAG and the relatively warm waters of the GSC gyre system (Figure 1b). Therefore the peak occurrence of *G. menardii* at Site 607 can be interpreted as representing small changes in the position of the two gyre systems. Apparently, peak influxes of *G. menardii* at Site 607 indicate intervals of enhanced northward heat transport.

[37] Little is known about the positioning and strength of past North Atlantic surface currents in relation to precession forcing. *Spaak* [1983] indicated that the strength of the Canary Current might have varied on a precession scale during the late Pliocene, possibly related to the strength of the trade winds. Direct evidence for variation in trade wind strength during MIS100 may come from the pollen data and terrigenous grain size measurements of ODP Site 658 [*Leroy and Dupont*, 1994]. These records reveal that the observed increase in the $\delta^{13}C_{benthos}$ record which we linked to MIS100.3 is accompanied by wetter climate conditions in northwest Africa and decreased NE trade wind strength. Further evidence that the precession cycle may have played a critical role on the strength of the trade winds during MIS100.3 comes from the n-alkane $\delta^{13}C$ record of the South Atlantic ODP Site 1083 [*Denison et al.*, 2005]. This Southern Hemisphere midlatitude record reflects relatively dry climate conditions (i.e., high contributions of C_4 plants and a high water stress of C_3 plants) during insolation cycle i-244, which clearly point to an opposite precession-related signal during i-244 as observed in northwest Africa. It was suggested that these climate conditions are triggered by reduced monsoonal precipitation in southwest Africa and are independent of glacial-interglacial variability [*Denison et al.*, 2005].

[38] In summary, MIS100.3 characterizes an interstadial phase during which precessional forcing may have resulted in (1) wetter climate conditions in the Mediterranean and northwest and northeast African regions related to a stronger summer monsoon circulation, (2) decreased NE trade wind strength along northwest Africa during winter due to a weaker Southern Hemisphere summer monsoon, and (3) the enhanced northward heat transport by surface currents, which are accompanied by a rejuvenation of the THC. The role of the precession cycle on the strength of the trade winds, and monsoonal precipitation has been extensively investigated by means of climate modeling experiments [i.e., *Kutzbach and Guetter*, 1986; *Tuenter et al.*, 2003], which confirm the patterns observed during MIS100.3. Recent climate modeling experiments further revealed that during minimum precession, the Atlantic overturning is stronger than during maximum precession [*Tuenter et al.*, 2005]. In the case where a vegetation module was incorporated in the model, maximum overturning lags precession by a few thousand years. *Tuenter et al.* [2005] showed that enhanced winter cooling in the region of NADW formation can be held responsible for the stronger convection in the North Atlantic Ocean during precession minima. A similar precession-forced mechanism could therefore explain a sudden rejuvenation of the Atlantic's conveyor during MIS100.3 and even the small time lag observed if vegetation feedbacks are taken into account. Hence the precession-driven increased transport of warm salty waters to the north during full glacial conditions may in turn have facilitated the melting of the large ice sheets, thereby triggering massive iceberg discharge. Subsequently, a reduction of the surface salinity conditions in the regions of deepwater formation may in turn shut down or reduce the THC. Such a feedback mechanism could therefore be responsible for the extreme cold (D-O) climate conditions observed at Site 981 and the central Mediterranean during MIS100.3.

[39] Although minimum precession values may have played a key role in triggering MIS100.3, a similar mechanism cannot explain MIS100.5. During MIS100.5, THC was most likely resumed after the first phase (MIS100.6) of ice sheet buildup during MIS100. Apparently, ice sheets were still not large enough to trigger massive iceberg discharge and hence North Atlantic and Mediterranean climate conditions returned to almost interglacial values. The apparent ~8-kyr spacing between MIS100.5 and MIS100.3 may point to a possible influence of astronomically modulated zonal wind-driven divergence in the eastern equatorial Atlantic on THC changes during MIS100 as proposed by *McIntyre and Molfino* [1996] for the late Pleistocene. *McIntyre and Molfino* [1996] propose a mechanism analogous to a long-period El Niño when the tropical easterlies diminish, surface waters are released from the Caribbean and Gulf of Mexico warm pool into the western boundary current of the North Atlantic subtropical gyre and, subsequently, into the subpolar Atlantic thereby producing the rapid melting of ice and hence Heinrich events. This modulation, which occurred on a period of 8.4 kyr over the past 45,000 years, is thought to be caused by the nonlinear response of climate to low-latitude insolation/precession forcing during minimum eccentricity, although it remains unclear why a periodicity of ~8.4 kyr, which would require a rather unusual precession period, should be important during the past 45 kyr [*Berger and Loutre*, 1997]. Nevertheless, the ~8-kyr time spacing between MIS100.5 and MIS100.3, the apparent ~8-kyr periodicity in the $\delta^{18}O_{G.ruber}$ record of Site 607, the minimum eccentricity values during MIS100 and the coincidence of MIS100.3 with minimum precession are not in disagreement with such a hypothesis. Data from piston core SU90-03 [*Chapman and Shackleton*, 1998] close to Site 607 indicate that during the past 45 kyr episodes of cold iceberg-laden waters alternate with the supply of warm saline waters from the subtopics. These changes are similar to our findings from MIS100, occurring on a semiprecession to H scale (5–8 kyr) and it was

concluded that cross-equatorial heat transport is a major factor controlling surface oceanography of the midlatitude North Atlantic [*Chapman and Shackleton*, 1998].

5. Summary and Conclusions

[40] Our results unambiguously demonstrate that millennial-scale cycles and associated Heinrich events are an intrinsic part of the climate system throughout the late Pliocene and Pleistocene notwithstanding the transition from the dominant 41-kyr to 100-kyr-controlled glacial cycles. Moreover, they show that the climate mechanisms responsible for the observed variations during MIS100 are very similar to those observed in the Pleistocene climate record. In particular, changes in North Atlantic SST, ice-rafted debris and strength of the THC are associated with a latitudinal migration of the polar front. The southward movement of this polar front in association with the maximum extension of Northern Hemisphere ice caps during stadial intervals influenced Mediterranean climate both directly by inflowing North Atlantic (polar) surface water (i.e., *N. atlantica* influxes) and indirectly by atmospheric disturbances (i.e., dust input). The presence of the subtropical planktonic foraminiferal species *G. menardii* during interstadial period MIS100.3 in the central North Atlantic indicates that the meridional heat flow from subtropical regions to the north increased, probably as a result of a precession-induced rejuvenation of the global THC. Such an astronomical-controlled mechanism however could not explain the occurrence of the 6–8 kyr older MIS100.5, unless a nonlinear response of the climate system to primary Milankovitch forcing may have played a critical role.

[41] **Acknowledgments.** We thank Hubert Vonhof, Gerald Gansen (Amsterdam Free University), and Monika Segel (Bremen University) for providing stable isotope facilities and the EU Project "Paleostudies" contract HPRI-CT-2001-0124 for financial support of isotope analyses. Hanneke Tijbosch and Wouter Kuiper assisted with foraminifer census counts and picking for isotopes. This research was carried out within the framework of the PIONEER program of F.J. Hilgen and VIDI program of L.J. Lourens, which are financially supported by the Netherlands Organization for Scientific Research (NWO).

References

Alley, R. B., and D. R. MacAyeal (1994), Ice-rafted debris associated with binge/purge oscillations of the Laurentide Ice Sheet, *Paleoceanography*, *9*, 503–511.

Asioli, A., F. Trincardi, J. J. Lowe, and F. Oldfield (1999), Short-term climate changes during the Last Glacial-Holocene transition: Comparison between Mediterranean records and the GRIP event stratigraphy, *J. Quat. Sci.*, *14*, 373–381.

Bard, E., F. Rostek, J.-L. Turon, and S. Gendreau (2000), Hydrological impact of Heinrich events in the subtropical northeast Atlantic, *Science*, *289*, 1321–1324.

Becker, J., F. J. Hilgen, L. J. Lourens, G.-J. Reichart, E. van der Laan, and T. J. Kouwenhofen (2005), Late Pliocene climate variability on Milankovitch to millennial time scales: A high-resolution study of MIS100 from the Mediterranean, *Palaeogeogr. Palaeoclimatol. Palaeoecol.*, *228*, 338–360.

Berger, A., and M.-F. Loutre (1997), Intertropical latitudes and precessional and half-precessional cycles, *Science*, *278*, 1476–1478.

Bickert, T., W. B. Curry, and G. Wefer (1997), Late Pliocene to Holocene (2.6–0 Ma) western equatorial Atlantic deep-water circulation: Inferences from benthic stable isotopes, *Proc. Ocean. Drill. Program Sci. Results*, *154*, 239–254.

Bond, G. C. (1992), Evidence for massive discharges of icebergs into the North Atlantic ocean during the last glacial period, *Nature*, *360*, 245–249.

Bond, G. C., W. Broecker, S. Johnsen, J. McManus, L. Labeyrie, J. Jouzel, and G. Bonani (1993), Correlations between climate records from North Atlantic sediments and Greenland ice, *Nature*, *365*, 143–147.

Bond, G. C., W. Showers, M. Elliot, M. Evans, R. Lotti, I. Hadjas, G. Bonani, and S. Johnson (1999), The North Atlantic's 1–2 kyr climate rhythm: Relation to Heinrich events, Dansgaard/Oescher cycles and the Little Ice Age, in *Mechanisms of Global Climate Change at Millennial Time Scales*, *Geophys. Monogr. Ser.*, vol. 112, edited P. U. Clark, R. S. Webb, and L. D. Keigwin, pp. 35–58, AGU, Washington, D. C.

Bond, G. C., B. Kromer, J. Beer, R. Muscheler, M. N. Evans, W. Showers, S. Hoffmann, R. Lotti-Bond, I. Hajdas, and G. Bonani (2001), Persistent solar influence on North Atlantic climate during the Holocene, *Science*, *294, 2130–2136.*

Broecker, W. (1992), Origin of the northern Atlantic's Heinrich events, *Clim. Dyn.*, *6*, 265–273.

Broecker, W. (1997), Thermohaline circulation, the Achilles Heel of our climate system: Will man-made CO_2 upset the current balance?, *Science*, *278*, 1582–1588.

Cacho, I., J. O. Grimalt, C. Pelejero, M. Canals, F. J. Sierro, J.-A. Flores, and N. J. Shackleton (1999), Dansgaard-Oeschger and Heinrich event imprints in Alboran Sea paleotemperatures, *Paleoceanography*, *14*, 698–705.

Cacho, I., J. O. Grimalt, F. J. Sierro, N. Shackleton, and M. Canals (2000), Evidence for enhanced Mediterranean thermohaline circulation during rapid climatic coolings, *Earth Planet. Sci. Lett.*, *183*, 417–429.

Cacho, I., J. O. Grimalt, M. Canals, and L. Sbaffi (2001), Variability of the western Mediterranean Sea surface temperature during the last 25,000 years and its connection with the Northern Hemisphere climatic changes, *Paleoceanography*, *16*, 40–52.

Channell, J. E. T., and B. Lehman (1999), Magnetic stratigraphy of North Atlantic sites 980–984, *Proc. Ocean Drill. Program Sci. Results*, *172*, 113–130.

Chapman, M. R., and N. J. Shackleton (1998), Millennial-scale fluctuations in North Atlantic heat flux during the last 150,000 years, *Earth Planet. Sci. Lett.*, *159*, 57–70.

Clement, A. C., R. Seager, and M. A. Cane (1999), Orbital controls on the El Niño/Southern Oscillation and the tropical climate, *Paleoceanography*, *14*, 441–456.

Combourieu-Nebout, N. (1991), Late Pliocene Northern Hemisphere glaciations: The continental and marine responses in the central Mediterranean, *Quat. Sci. Rev.*, *10*, 319–334.

Combourieu-Nebout, N., J. L. Touron, R. Zahn, L. Capotondi, L. Londeix, and K. Pahnke (2002), Enhanced aridity and atmospheric high-pressure stability over the western Mediterranean during the North Atlantic cold events of the past 50 k. y., *Geology*, *30*, 863–866.

Cortijo, E., L. Labeyrie, L. Vidal, M. Vautravers, M. Chapman, J.-C. Duplessy, M. Elliot, M. Arnold, J.-L. Turon, and G. Auffret (1997), Changes in sea surface hydrology associated with Heinrich event 4 in the North Atlantic Ocean between 40 an 60°N, *Earth Planet. Sci. Lett.*, *146*, 29–45.

Curry, W. B., and D. W. Oppo (2005), Glacial water mass geometry and the distribution of $\delta^{13}C$ of ΣCO_2 in the western Atlantic Ocean, *Paleoceanography*, *20*, PA1017, doi:10.1029/2004PA001021.

Dannenmann, S., B. K. Linseley, D. W. Oppo, Y. Rosenthal, and L. Beaufort (2003), East Asian monsoon forcing of suborbital variability in the Sulu Sea during marine isotope stage 3: Link to Northern Hemisphere climate, *Geochem. Geophys. Geosyst.*, *4*(1), 1001, doi:10.1029/2002GC000390.

Dansgaard, W., et al. (1993), Evidence for general instability of past climate from a 250-kyr ice-core record, *Nature*, *364*, 218–220.

Denison, S. M., M. A. Maslin, C. Boot, R. D. Pancost, and V. J. Ettwein (2005), Precession-forced changes in south west African vegetation during marine isotope stages 101–100 (~2.56–2.51 Ma), *Palaeogeogr. Palaeoclimatol. Palaeoecol.*, *220*, 375–386.

Dokken, T. M., and E. Jansen (1999), Rapid changes in the mechanism of ocean convection during the last glacial period, *Nature*, *401*, 458–461.

Draut, A., M. E. Raymo, J. F. McManus, and D. W. Oppo (2003), Climate stability during the Pliocene warm period,

Paleoceanography, *18*(4), 1078, doi:10.1029/2003PA000889.

Flower, B. P. (1999), *Data report*: Planktonic foraminifers from the subpolar North Atlantic and Nordic Seas, sites 980–987 and 907, *Proc. Ocean Drill. Program Sci. Results*, *172*, 19–34.

Heinrich, H. (1988), Origin and consequences of cyclic ice rafting in the NE Atlantic Ocean during the past 130,000 years, *Quat. Res.*, *29*, 142–152.

Henrich, R., and K.-H. Baumann (1994), Evolution of the Norwegian current and the Scandinavian ice sheets during the past 2.8 My: Evidence from ODP Leg 104 biogenic carbonate and terrigenous records, *Palaeogeogr. Palaeoclimatol. Palaeoecol.*, *108*, 75–94.

Henrich, R., K.-H. Baumann, R. Huber, and H. Meggers (2002), Carbonate preservation records of the past 3 Myr in the Norwegian-Greenland Sea and the northern North Atlantic: Implications for the history of NADW production, *Mar. Geol.*, *184*, 17–39.

Hilbrecht, H. (1996), Extant planktic foraminifera and the physical environment in the Atlantic and Indian oceans, *Mitt. Geol. Inst. Eidgen 300*, 93 pp., Tech. Hochsch., Zürich, Switzerland. (Available at http://www.ngdc.noaa.gov/mgg/geology/hh1996/)

Jansen, E., M. E. Raymo, P. Blum, and T. D. Herbert (1996a), Sites 980/981, *Proc. Ocean Drill. Program Initial Rep.*, *162*, 81–138.

Jansen, E., M. E. Raymo, P. Blum, and T. D. Herbert (1996b), Explanatory notes, Proc. Ocean Drill, *Program Initial Rep.*, *162*, 49–90.

Kleiven, H. F., E. Jansen, T. Fronval, and T. M. Smith (2002), Intensification of Northern Hemisphere glaciations in the circum Atlantic region (3.5–2. 4 Ma)—Ice-rafted detritus evidence, *Palaeogeogr. Palaeoclimatol. Palaeoecol.*, *184*, 213–223.

Kutzbach, J. E., and P. J. Guetter (1986), The influence of changing orbital parameters and surface boundary conditions on climate simulations for the past 18000 years, *J. Atmos. Sci.*, *43*(16), 1726–1759.

Larrasoaña, J. C., A. P. Roberts, E. J. Rohling, M. Winkelhofer, and R. Wehausen (2003), Three million years of monsoon variability over the northern Sahara, *Clim. Dyn.*, *21*, 689–698.

Leroy, S., and L. Dupont (1994), Development of vegetation and continental aridity in northwestern Africa during the late Pliocene: The pollen record of ODP Site 658, *Palaeogeogr. Palaeoclimatol. Palaeoecol.*, *109*, 295–316.

Leuschner, D. C., and F. Sirocko (2000), The low-latitude monsoon climate during Dansgaard-Oeschger cycles and Heinrich events, *Quat. Sci. Rev.*, *19*, 243–254.

Lourens, L. J., F. J. Hilgen, J. Gudjonsson, and W. J. Zachariasse (1992), Late Pliocene to early Pleistocene astronomically-forced sea surface productivity and temperature variations in the Mediterranean, *Mar. Micropaleontol.*, *19*, 49–78.

Lourens, L. J., A. Antonarakou, F. J. Hilgen, A. A. M. Van Hoof, C. Vergnaud-Grazzini, and W. J. Zachariasse (1996), Evaluation of the Plio-Pleistocene astronomical timescale, *Paleoceanography*, *11*, 391–413.

Lourens, L. J., R. Wehausen, and H. J. Brumsack (2001), Geological constraints on tidal dissipation and dynamical ellipticity of the Earth over the past three million years, *Nature*, *409*, 1029–1032.

MacAyeal, D. R. (1993), Binge/purge oscillations of the Laurentide ice sheet as a cause of the North Atlantic's Heinrich events, *Paleoceanography*, *8*, 775–784.

Marchitto, T. M., W. B. Curry, and D. W. Oppo (1998), Millennial-scale changes in North Atlantic circulation since the last glaciation, *Nature*, *393*, 557–561.

McIntyre, A., and B. Molfino (1996), Forcing of Atlantic equatorial and subpolar millennial cycles by precession, *Science*, *274*, 1867–1870.

McIntyre, K., M. L. Delaney, and A. C. Ravelo (2001), Millennial-scale climate change and oceanic processes in the late Pliocene and early Pleistocene, *Paleoceanography*, *16*, 535–543.

Meggers, H., and K.-H. Baumann (1997), Contributions to the Micropaleontology and Paleoceanography of the Northern North Atlantic, *Grzybowski Found. Spec. Publ.*, vol. 5, edited by H. C. Hass and M. A. Kaminski, pp. 39–50, Grzybowski Found., Krakow.

Mix, A. C., N. G. Pisias, W. Rugh, J. Wilson, A. Morey, and T. K. Hagelberg (1995), Benthic foraminifer stable isotope record from Site 849 (0–5 Ma): Local and global climate changes, *Proc. Ocean. Drill. Program Sci. Results*, *138*, 371–412.

Moreno, A., I. Cacho, M. Canals, M. A. Prins, M. F. Sanchez-Goñi, J. O. Grimalt, and G.-J. Weltje (2002), Saharan dust transport and high-latitude glacial climate variability: The Alboran Sea record, *Quat. Res.*, *58*, 318–328.

Moreno, A., I. Cacho, M. Canals, J. O. Grimalt, and A. Sanchez-Vidal (2004), Millennial-scale variability in the productivity signal from the Alboran Sea record, western Mediterranean Sea, *Palaeogeogr. Palaeoclimatol. Palaeoecol.*, *211*, 205–219.

Ortiz, J., A. Mix, S. Harris, and S. O'Connell (1999), Diffuse spectral reflectance as a proxy for percent carbonate content in the North Atlantic sediments, *Paleoceanography*, *14*, 171–186.

Ottens, J. J. (1991), Planktic foraminifera as North Atlantic water mass indicators, *Oceanol. Acta*, *14*, 123–140.

Otterman, J., J. K. Angell, J. Ardizzone, R. Atlas, S. Schubert, and D. Starr (2002), North-Atlantic surface winds examined as the source of winter warming in Europe, *Geophys. Res. Lett.*, *29*(19), 1912, doi:10.1029/2002GL015256.

Peterson, L. C., G. H. Haug, K. A. Hughen, and U. Röhl (2000), Rapid changes in the hydrologic cycle of the tropical Atlantic during the last glacial, *Science*, *290*, 1947–1951.

Poore, R. Z., and W. A. Berggren (1975), The morphology and classification of *Neogloboquadrina atlantica* (Berggren), *J. Foraminiferal Res.*, *5*, 692–694.

Raymo, M. E. (1992), Global climate change: A three million year perspective, in *Start of a Glacial, Proceedings of the Mallorca NATO ARW*, edited by G. Kukla and E. Went, pp. 207–223, Springer, New York.

Raymo, M. E., W. F. Ruddiman, and B. M. Clement (1986), Pliocene-Pleistocene paleoceanography of the North Atlantic at Deep Sea Drilling Project Site 609, *in Initial Rep Deep Sea Drill. Proj.*, *94*, 895–901.

Raymo, M. E., W. F. Ruddiman, J. Backman, B. M. Clement, and D. G. Martinson (1989), Late Pliocene variation in Northern Hemisphere ice sheets and North Atlantic deep water circulation, *Paleoceanography*, *4*, 413–446.

Raymo, M. E., W. F. Ruddiman, N. J. Shackleton, and D. W. Oppo (1990), Evolution of Atlantic-Pacific $\delta^{13}C$ gradients over the last 2.5. m. y., *Earth Planet. Sci. Lett.*, *97*, 353–368.

Raymo, M. E., D. Hodell, and E. Jansen (1992), Response of deep ocean circulation to initiation of Northern Hemisphere glaciation (3–2 Ma), *Paleoceanography*, *7*, 645–672.

Raymo, M. E., K. Ganley, S. Carter, D. W. Oppo, and J. McManus (1998), Millennial-scale climate instability during the early Pleistocene epoch, *Nature*, *392*, 699–702.

Raymo, M. E., D. W. Oppo, B. P. Flower, D. A. Hodell, J. F. McManus, K. A. Venz, H. F. Kleiven, and K. McIntyre (2004), Stability of North Atlantic water masses in face of pronounced climate variability during the Pleistocene, *Paleoceanography*, *19*, PA2008, doi:10.1029/2003PA000921.

Robinson, L. F., J. F. Adkins, L. D. Keigwin, J. Southon, D. P. Fernandez, S.-L. Wang, and D. S. Scheirer (2005), Radiocarbon variability in the western North Atlantic during the last deglaciation, *Science*, *310*, 1469–1473.

Robinson, S. G., M. A. Maslin, and N. McCave (1995), Magnetic susceptibility variations in upper Pleistocene deep-sea sediments of the NE Atlantic: Implications for ice rafting and paleocirculation at the last glacial maximum, *Paleoceanography*, *10*, 221–250.

Rohling, E. J., A. Hayes, S. De Rijk, D. Kroon, W. J. Zachariasse, and D. Eisma (1998), Abrupt cold spells in the northwest Mediterranean, *Paleoceanography*, *13*, 316–322.

Ruddiman, W. F., A. McIntyre, and M. Raymo (1986), Paleoenvironmental results from North Atlantic sites 607 and 609, *Initial Rep. Deep Sea Drill.*, 855–878.

Ruddiman, W. F., M. E. Raymo, D. G. Martinson, B. M. Clement, and J. Backman (1989), Pleistocene evolution of Northern Hemisphere climate, *Paleoceanography*, *4*, 353–412.

Sanchez-Goñi, M. F., I. Cacho, J. L. Turon, J. Guiot, F. J. Sierro, J.-P. Peypouquet, J. O. Grimalt, and N. J. Shackleton (2002), Synchroneity between marine and terrestrial responses to millennial scale climatic variability during the last glacial period in the Mediterranean region, *Clim. Dyn.*, *19*, 95–105.

Sarnthein, M., et al. (1995), Variations in Atlantic surface ocean paleoceanography, 50°–80°N: A time-slice record of the last 30,000 years, *Paleoceanography*, *10*, 1063–1094.

Schmidt, G. A., and S. Mulitza (2002), Global calibration of ecological models for planktic foraminifera from coretop carbonate oxygen-18, *Mar. Micropaleontol.*, *44*, 125–140.

Schmittner, A., and A. C. Clement (2002), Sensitivity of the thermohaline circulation to tropical and high latitude freshwater forcing during the last glacial-interglacial cycle, *Paleoceanography*, *17*(2), 1017, doi:10.1029/2000PA000591.

Schmitz, W. J. Jr., and M. S. McCartney (1993), On the North Atlantic circulation, *Rev. Geophys.*, *31*, 29–49.

Seidov, D., and M. A. Maslin (1999), North Atlantic deep water circulation collapse during Heinrich events, *Geology*, *27*, 23–26.

Shackleton, N. J., and M. A. Hall (1984), Oxygen and carbon isotope stratigraphy of Deep Sea Drilling Project Hole 552A: Plio-Pleistocene glacial history, *Initial Rep. Deep Sea Drill. Proj.*, *74*, 599–609.

Shackleton, N. J., and N. D. Opdyke (1976), Oxygen isotope and paleomagnetic stratigraphy of Pacific core V28–238 late Pliocene to latest Pleistocene, *Mem. Geol. Soc. Am.*, *145*, 449–464.

Shackleton, N. J., M. A. Hall, and D. Pate (1995), Pliocene stable isotope stratigraphy of ODP Site 846, *Proc. Ocean. Drill. Program Sci. Results*, *138*, 337–356.

Spaak, P. (1983), Accuracy in correlation and ecological aspects of the planktonic foraminiferal zonation of the Mediterranean Pliocene, *Utrecht Micropaleontol. Bull.*, *28*, 168 pp.

Stott, L., C. Poulsen, S. Lund, and R. Thunell (2002), Super ENSO and global climate oscillations at millennial time scales, *Science*, *297*, 2345–2348.

Tiedemann, R. (1991), Acht Millionen Jahre Klimageschichte von Nordwest Afrika und Paläozeanographie des angrenzenden Atlantiks: Hochauflösende Zeitreihen von ODP-Sites 658–661, *Ber. 46*, 190 pp., Univ. zu Kiel, Kiel, Germany.

Tuenter, E., S. L. Weber, F. J. Hilgen, and L. J. Lourens (2003), The response of the African summer monsoon to remote and local forcing due to precession and obliquity, *Global Planet. Change*, *36*(4), 219–235.

Tuenter, E., S. L. Weber, F. J. Hilgen, L. J. Lourens, and A. Ganopolski (2005), Simulation of climate phase lags in response to precession and obliquity forcing and the role of vegetation, *Clim. Dyn.*, *24*, 279–295.

van Os, B. J. H., L. J. Lourens, L. Beaufort, F. J. Hilgen, and G. J. de Lange (1994), The formation of Pliocene sapropels and carbonate cycles in the Mediterranean: Diagenesis, dilution, and productivity, *Paleoceanography*, *15*, 425–442.

Versteegh, G. J. M. (1997), The onset of major Northern Hemisphere glaciations and their impact on dinoflagellate cysts and acritarchs from the Singa section, Calabria (southern Italy) and DSDP Holes 607/607A (North Atlantic), *Mar. Micropaleontol.*, *30*, 319–343.

Voelker, A., and Workshop Participants (2002), Global distribution of centennial-scale records during marine isotope stage (MIS) 3: A database, *Quat. Sci. Rev.*, *21*, 1185–1212.

Wara, M. W., A. C. Ravelo, and J. S. Revenaugh (2000), The pacemaker always rings twice, *Paleoceanography*, *15*, 616–624.

Wehausen, R. (1999), Anorganische Geochemie zyklischer Sedimente aus dem östlichen Mittelmeer: Rekonstruktion der Paläoumweltbedingungen, Dissertation thesis, 162 pp., Carl-von-Ossietzky-Univ. of Oldenburg, Oldenburg, Germany.

Willis, K. J., A. Kleckowski, and S. J. Crowhurst (1999), 124,000-year periodicity in terrestrial vegetation change during the late Pliocene epoch, *Nature*, *397*, 685–688.

Zachariasse, W. J., L. Gudjonsson, F. J. Hilgen, L. J. Lourens, P. J. J. M. Verhallen, C. G. Langereis, and J. D. A. Zijderveld (1990), Late Gauss to early Matuyama invasions of *Neogloboquadrina atlantica* in the Mediterranean and associated record of climatic change, *Paleoceanography*, *5*, 239–252.

J. Becker, School of Earth, Ocean and Planetary Sciences, Cardiff University, Park Place, Cardiff CF10 3YE, U.K. (beckerj@cardiff.ac.uk)

L. J. Lourens, Department of Earth Sciences, Faculty of Geosciences, Utrecht University, Budapestlaan 4, 3584 CD Utrecht, Netherlands.

M. E. Raymo, Department of Earth Sciences, Boston University, 685 Commonwealth Avenue, Boston, MA 02215, USA.